J MATER RES TECHNOL. 2019;xxx(xx):xxx–xxx

Available online at www.sciencedirect.com

jmr&t Journal of Materials Research and Technology

www.jmrt.com.br

Original Article

Stability analysis and multiple solution of $Cu–Al_2O_3/H_2O$ nanofluid contains hybrid nanomaterials over a shrinking surface in the presence of viscous dissipation

Liaquat Ali Lund[a], *Zurni Omar*[a], *Ilyas Khan*[b,*], *Asiful H. Seikh*[c], *El-Sayed M. Sherif*[c,d], *Kottakkaran Sooppy Nisar*[e]

[a] *School of Quantitative Sciences, Universiti Utara Malaysia, 06010 Sintok, Kedah, Malaysia*

[b] *Faculty of Mathematics and Statistics, Ton Duc Thang University, Ho Chi Minh City, Viet Nam*

[c] *Centre of Excellence for Research in Engineering Materials, King Saud University, P.O. Box-800, Riyadh 11421, Saudi Arabia*

[d] *Electrochemistry and Corrosion Laboratory, Department of Physical Chemistry, National Research Centre, El-Behoth St. 33, Dokki, Cairo 12622, Egypt*

[e] *Department of Mathematics, College of Arts and Science, Prince Sattam bin Abdulaziz University, Wadi Al-Dawaser 11991, Saudi Arabia*

ARTICLE INFO

Article history:
Received 15 October 2019
Accepted 27 October 2019
Available online xxx

Keywords:
Hybrid nanomaterials
Nanofluid
Dual solutions
Stability analysis
Viscous dissipation
Shrinking surface

ABSTRACT

Researchers are using different types of nanomaterials for the enhancement of the thermal performance of regular fluids such as water, kerosene oil, etc. However, these days, the researchers are more interested in hybrid nanomaterials. The purpose of this communication is to examine the stability analysis of $Cu–Al_2O_3$/water hybrid nanofluid over a non-linear shrinking sheet. The hybrid nanomaterials are composed of Cu and Al_2O_3. These hybridized nanomaterials are then dissolved in water taken as base fluid to form $Cu–Al_2O_3$//water hybrid nanofluid. Mathematical analysis and modeling have been attended in the presence of viscous dissipation and suction/injection effects. The governing equations of mathematical models are transformed into self-similar solutions in the form of ODEs by using similarity transformation. Solutions of the non-linear ODEs are created by employing of three-stage Lobatto IIIa formula which is built-in BVP4C function in the MATLAB software. A comparison of the current study has been done with the preceding published literature. The distributions of velocity, temperature profiles, coefficient of skin friction and heat transfer rate are presented graphically and conferred for numerous significant parameters entering into the problem. Results revealed the existence of dual solutions for a certain range of the suction/blowing parameter. Stability analysis is also done in order to obtain dual solutions stability. The smallest eigenvalues suggest that the first solution is stable from the second solution. Hybrid nanomaterials have a high scope toward nurturing our day-to-day life.

* *Corresponding author.*
E-mail: ilyaskhan@tdtu.edu.vn (I. Khan).

https://doi.org/10.1016/j.jmrt.2019.10.071

Please cite this article in press as: Lund LA, et al. Stability analysis and multiple solution of $Cu–Al_2O_3/H_2O$ nanofluid contains hybrid nanomaterials over a shrinking surface in the presence of viscous dissipation. J Mater Res Technol. 2019. https://doi.org/10.1016/j.jmrt.2019.10.071

Nomenclature

u, v	velocity components
C_f	skin friction coefficient
Cu	copper
Al_2O_3	alumina
Nu_x	local Nusselt number
k_{nf}	thermal conductivity of the nanofluid
T	temperature
T_0	a constant
T_w	variable temperature at the sheet
T_∞	ambient temperature
m	positive constant
b	suction and blowing parameter
N_u	local Nusselt number
Ec	Eckert number
γ	smallest eigenvalue
τ	Stability transformed variable
k_{hnf}	thermal conductivity of the hybrid nanofluid
α	thermal diffusivity
Pr	Prandtl number
v_w	suction/injection velocity
$u_w(x)$	velocity of shrinking surface
$(\rho c_p)_{hnf}$	heat capacitance of the hybrid nanofluid
ρ_{hnf}	effective density of the hybrid nanofluid
μ_{hnf}	effective dynamic viscosity of the hybrid nanofluid
η	transformed variable
ϕ	nanoparticle volume fraction

1. Introduction

In the present century, enhancement of heat transfer is a very interesting subject to discuss due to its various applications in engineering and industries. Many applications of industries are required high thermal conductivity but there is no such regular fluid. Fluids like oil, ethylene glycol and water possess low thermal conductivity and cannot be used in many applications. Due to this drawback, a new kind of fluid has been introduced by Choi and Eastman [1] in 1995 which is nanofluid to improve thermal efficiency. It is composed of the dispersed nanometer-sized particles and base liquid. The examination of nanofluids is useful in heat exchangers, thermal engineering, biomedicine, cancer therapy, electronic chemical process, etc. Nanofluids have good heat transfer characteristics as compared to ordinary regular fluids and possess the new kind of production coolants. It is proved now that the thermal conductivity of nanofluid is significantly high and therefore important applications to microscale cooling are noticeable. Especially the nanofluids model of single-phase flow is significant in lubricants, coolants, and also in daily life applications such as mobile computer processors, air-conditioning, refrigeration, microelectronics, etc. In industrial science, heating development can be easily gotten from solar thermal energy which is friendly and convenient. A process that changes the radiations of solar into heat energy is known as a solar collector. For boosting up the effectiveness of these collectors, oil, ethylene glycol and water are substituted in nanofluids. In the last two decades are witnessed the great developments in nanofluids, many researchers studied nanofluid numerically and experimentally. Gherasim et al. [2] examined the nanofluid experimentally by considering the water as a base fluid and particles of alumina as nanoparticles. They found that heat transfer is increased in radial flow cooling systems. Chandrasekar et al. [3] investigated the thermal conductivity of alumina water-based nanofluid by using of Maxwell and Einstein models. They kept the diameters of nanoparticles 43 nm and found that viscosity and thermal conductivity of nanofluid are directly proportional to each other. Nanofluids containing graphene oxide nanosheets were studied by Yu et al. [4] in which it was seen that thermal conductivity increased in the range 5.0–30.2 vol% when base fluid was distilled water. Dalkılıç et al. [5] carried out the study on water-based hybrid nanofluid in which they considered graphite and alumina as the solid particles. TiO_2–MWCNTs–water hybrid nanofluid was experimentally examined by Akhgar and Toghraie [6]. They used two models and found that thermal conductivity is maximized in 38.7%. Moreover, Esfahani and Toghraie [7] investigated silica/water–ethylene glycol and found that maximum thermal conductivity is produced when volume fraction is 5%. Some more related experimental and numerical works on nanofluids and hybrid nanofluids and their applications can be seen in these articles [8–19].

As it is mentioned that many researchers considered the numerical approach to understanding the behavior of nanofluids. There are two mathematical models in which the numerical approach can be used easily, the first one is Tiwari and Das's model [20] and the second one is Buongiorno's model [21]. Hayat et al. [22] used Tiwari and Das's model to investigate the stagnation point flow of nanofluid in presence of thermal radiation effect. They considered water as a base fluid and carbon nanotubes as a solid material and noticed that temperature and melting parameter are inversely proportional to each other. Alrashed et al. [23] also considered same model and examined nanofluid by numerical approach. Further, temperature of surface reduced for higher values of Reynolds number. Other related articles of Tiwari and Das's model [20] have been used by many researchers in their studies (refer [24–35]). Farooq et al. [36] considered Buongiorno's model in their studies for non-Newtonian nanofluid with effect of thermal radiation and magnetic field. It is stated that thickness of concentration profiles decreased as Brownian motion of materials are enhanced. The same model is considered for cross nanofluid by Khan et al. [37] in which they also investigated the effect of activation energy on the various profiles. Further, Hayat et al. [38–44], Khan et al. [45–47], Rasool and Zhang [48], Khan et al. [49], Lund et al. [50], Ullah et al. [51], Rasool et al. [52], Lund et al. [53], Sheremet et al. [54] used Buongiorno's model in their studies and investigated the effect of Brownian motion and thermophoresis effect on the temperature of various nanofluids. A few more interesting works on Buongiorno's model can be seen in these articles [55–57]. It is worth to highlight that most of the above studies have been done for single solutions so far. The present study aims to determine the multiple solutions by considering Tiwari and Das's model. In recent years, it can be seen in the published literature of heat transfer enhancement, researchers are inter-

Please cite this article in press as: Lund LA, et al. Stability analysis and multiple solution of Cu–Al_2O_3/H_2O nanofluid contains hybrid nanomaterials over a shrinking surface in the presence of viscous dissipation. J Mater Res Technol. 2019. https://doi.org/10.1016/j.jmrt.2019.10.071

Table 1 – Thermophysical properties of hybrid nanofluid [63,77].

Properties	Hybrid nanofluid
Dynamic viscosity	$\mu_{hnf} = \frac{\mu_f}{(1-\phi_{Cu})^{2.5}(1-\phi_{Al_2O_3})^{2.5}}$
Density	$\rho_{hnf} = (1+\phi_{Al_2O_3})[(1-\phi_{Cu})\rho_f + \phi_{Cu}\rho_{Cu}] + \phi_{Al_2O_3}\rho_{Al_2O_3}$
Thermal conductivity	$k_{hnf} = \frac{k_{Al_2O_3}+2k_{nf}-2\phi_{Al_2O_3}(k_{nf}-k_{Al_2O_3})}{k_{Al_2O_3}+2k_{nf}+\phi_{Al_2O_3}(k_{nf}-k_{Al_2O_3})} \times (k_{nf})$where $k_{nf} = \frac{k_{Cu}+2k_f-2\phi_{Cu}(k_f-k_{Cu})}{k_{Cu}+2k_f+\phi_{Cu}(k_f-k_{Cu})} \times (k_f)$
Heat capacity	$(\rho c_p)_{hnf} = (1+\phi_{Al_2O_3})[(1-\phi_{Cu})(\rho c_p)_f + \phi_{Cu}(\rho c_p)_{Cu}] + \phi_{Al_2O_3}(\rho c_p)_{Al_2O_3}$

ested to find the better kind of fluids instead of single-phase and two-phase nanofluids. Regarding this, in order to get high thermal conductivity a new kind of nanofluid has been introduced namely 'hybrid nanofluid'. Hybrid nanofluid can be defined as it is the kind of nanofluid in which two different kinds of nanoparticles dissolve in the single base fluid. It has been observed that it produces excellent thermal conductivity as compared to base fluid and nanofluid containing single nanoparticles. These kinds of fluids can be used in many fields of heat transfer such as generator cooling, electronic cooling, nuclear system cooling, the coolant in machining, drug reduction, etc. Due to the interesting behavior of hybrid nanofluids in rising characteristics of heat conductivity attracts the many researchers to consider hybrid nanofluids in their studies to deal with real problems of the word. Sheikholeslami et al. [58] considered the hybrid nanofluid in the circular cavity. Arasteh et al. [59] investigated the hybrid nanofluid and found that increments in metal foams rise the temperature gradient. Devi and Devi [60] considered the hybrid nanofluid over the stretching surface in the presence of the magnetic effect. After one year, Devi and Devi [61] examined another hybrid nanofluid by a mathematical approach. They compared their results with experimental results and found in the excellent agreement. In their study, water is base fluid and alumina and copper are solid nanoparticles and they found that heat transfer of hybrid nanofluid is higher than the nanofluid containing single nanoparticles. Hybrid nanofluid for multiple solutions was studied by Waini et al. [62] in which they successfully found the dual solutions. Further, they also performed stability analysis and determined that only the first solution is the stable one. In the same year, Waini et al. [63] also considered another kind of hybrid nanofluid over the vertical thin needle and obtained the dual solutions.

The motivation behind this investigation is the above studies in which numerous researchers considered different base fluid along with different nanoparticles and found interesting behavior of heat characteristics. Very few researchers attempted to find the multiple solutions of hybrid nanofluids. In this study, we examine the problem of steady flow and heat transfer of hybrid nanofluid over the non-linear shrinking surface with the effect of viscous dissipation and wall mass suction. For that purpose, Tiwari and Das [20] have been employed in the equations of nanofluid by considering water as a base fluid and two different nanoparticles namely alumina and copper. The main aims of this paper are to advance the steady flow of hybrid nanofluid toward the non-linear shrinking surface into five directions. Firstly, to obtain multiple solutions by employing of numerical method in MATLAB software. Secondly, to predict the effect of hybrid nanofluid in both solutions. Thirdly, to examine the effect of viscous dissipations. Fourth, to analyze the nanoparticles (alumina and copper) effects for pure water base fluid. Fifth, to perform stability analysis for indicating the stable solution.

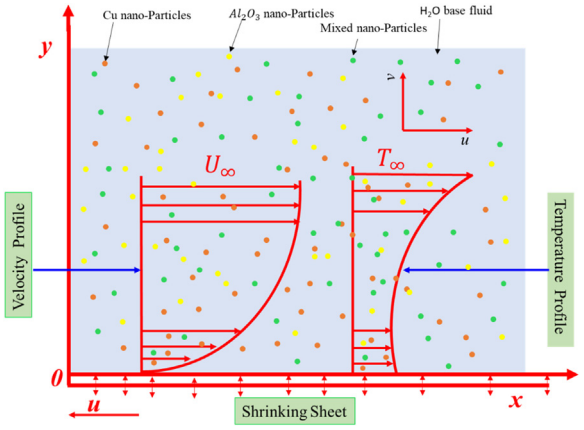

Fig. 1 – Physical model and coordinate systems.

2. Problem formulation

Let us consider the steady incompressible hybrid nanofluid flow on a shrinking surface with the effect of viscous dissipation. Water is considered as a base fluid copper and alumina nanoparticles. Fig. 1 shows the physical model of the problem. The velocity of shrinking surface is $u_w(x) = -cx^m$ where c is positive constant. On the other hand, mass flux velocity is also considered as $v_w(x) = -b\sqrt{c\vartheta}x^{(m-1)/2}$. Temperature inside the boundary layer is $T_w = T_\infty + T_0x^{2m}$ and outside the boundary layer is T_∞. Hybrid nanofluid is considered in which the size of nanoparticles is uniform. By considering the above assumptions, boundary layer equations can be written in the model of Tiwari and Das [20] as follows

$$\frac{\partial u}{\partial x} + \frac{\partial v}{\partial y} = 0 \tag{1}$$

$$u\frac{\partial u}{\partial x} + v\frac{\partial u}{\partial y} = \frac{\mu_{hnf}}{\rho_{hnf}}\frac{\partial^2 u}{\partial y^2} \tag{2}$$

$$u\frac{\partial T}{\partial x} + v\frac{\partial T}{\partial y} = \frac{k_{hnf}}{(\rho c_p)_{hnf}}\frac{\partial^2 T}{\partial y^2} + \frac{\mu_{hnf}}{(\rho c_p)_{hnf}}\left(\frac{\partial u}{\partial y}\right)^2 \tag{3}$$

The subjected boundary conditions are

$$\begin{cases} v = v_w(x), \quad u = u_w(x), \quad T = T_w \text{ as } y \to 0 \\ u \to 0, \quad T \to T_\infty \text{ as } y \to \infty \end{cases} \tag{4}$$

Please cite this article in press as: Lund LA, et al. Stability analysis and multiple solution of Cu–Al_2O_3/H_2O nanofluid contains hybrid nanomaterials over a shrinking surface in the presence of viscous dissipation. J Mater Res Technol. 2019. https://doi.org/10.1016/j.jmrt.2019.10.071

Table 2 – The thermo physical properties of the base fluid (water) and the nanoparticles [63,78].

Fluids	ρ (kg/m^3)	c_p (J/kg K)	k (W/m K)
Alumina (Al_2O_3)	3970	765	40
Copper (Cu)	8933	385	400
Water (H_2O)	997.1	4179	0.613

where respective velocities of x-axis and y-axis are u and v and T stands for temperature. Further, k_{hnf}, μ_{hnf}, ρ_{hnf} and $(\rho c_p)_{hnf}$ are the thermal conductivity, the dynamic viscosity, the density, and heat capacity of the hybrid nanofluid respectively. Further, subscript *hnf* indicates the hybrid nanofluid thermophilic properties. In this study, we follow the special form of thermophysical properties of Waini et al. [63] in order to examine the flow model. Table 1 is given for the thermophysical properties of hybrid nanofluid which will be used in this study. Moreover, Table 2 is constructed for the thermophysical properties of nanoparticles and base fluid.

Now, following similarity transformations are used to convert PDEs into ODEs.

$$\begin{cases} v = -\sqrt{\dfrac{c\vartheta(m+1)}{2}}x^{(m-1)/2}\left[f(\eta)+\dfrac{m-1}{m+1}\eta f'(\eta)\right] \\ u = cx^m f'(\eta),\ \eta = y\sqrt{\dfrac{c(m+1)}{2\vartheta}}x^{(m-1)/2} \\ \theta(\eta) = (T-T_\infty)/(T_w-T_\infty) \end{cases} \tag{5}$$

Substituting Eq. (5) in Eqs. (1)–(3), Eq. (1) is automatically satisfied and Eqs. (2) and (3) take the following dimensionless form

$$\xi_1 f''' + f''f - \frac{2m}{(m+1)}(f')^2 = 0 \tag{6}$$

$$\frac{\xi_2}{Pr}\theta'' + \theta' f - \frac{4m}{(m+1)}\theta f' + \xi_3 Ec(f'')^2 = 0 \tag{7}$$

Subject to boundary conditions

$$\begin{cases} f(0) = -b\sqrt{\dfrac{2}{m+1}},\quad f'(0) = -1,\quad \theta(0) = 1 \\ f'(\eta)\to 0,\quad \theta(\eta)\to 0 \text{ as } \eta\to\infty \end{cases} \tag{8}$$

Here, prime denotes differentiation due to η; the Prandtl number $Pr = \vartheta_f/\alpha_f$ and Eckert number $Ec = c^2\rho_f/T_0(\rho c_p)_f$, b is the suction parameter ($b<0$) and injection parameter ($b>0$).

The physical quantities of interest are the coefficient of skin friction C_f and Nusselt number Nu_x which can be defined as

$$C_f = \frac{\mu_{hnf}}{\rho_f u_w^2}\left(\frac{\partial u}{\partial y}\right)|y=0,\quad Nu_x = -\frac{xk_{hnf}}{k_f(T_w-T_\infty)}\left(\frac{\partial T}{\partial y}\right)|y=0 \tag{10}$$

By applying Eq. (9) in Eq. (10), we have

$$\begin{aligned} &\sqrt{Re}C_f = \frac{1}{(1-\phi_{Cu})^{2.5}(1-\phi_{Al_2O_3})^{2.5}}\sqrt{\frac{(m+1)}{2}}f''(0); \\ &\sqrt{\frac{1}{Re}}Nu_x = -\frac{k_{hnf}}{k_f}\sqrt{\frac{(m+1)}{2}}\theta'(0) \end{aligned} \tag{11}$$

where Re is local Reynold number.

3. Stability analysis

The study of stability analysis was carried out by Merkin [64] and kept continue by many other researchers in their studies [65–69]. According to them, the ordinary (similarity) equations possess multiple solutions where first (second) or upper (lower) solutions are always stable (unstable). In order to test these features, the governing Eqs. (2) and (3) are changed to unsteady form by introducing new time-dependent similarity variable $\tau = cx^{m-1}t$, we get

$$\frac{\partial u}{\partial t} + u\frac{\partial u}{\partial x} + v\frac{\partial u}{\partial y} = \frac{\mu_{hnf}}{\rho_{hnf}}\frac{\partial^2 u}{\partial y^2} \tag{12}$$

$$\frac{\partial T}{\partial t} + u\frac{\partial T}{\partial x} + v\frac{\partial T}{\partial y} = \frac{k_{hnf}}{(\rho c_p)_{hnf}}\frac{\partial^2 T}{\partial y^2} + \frac{\mu_{hnf}}{(c\rho_p)_{hnf}}\left(\frac{\partial u}{\partial y}\right)^2 \tag{13}$$

The new similarity variables are now

$$\begin{cases} v = -\sqrt{\dfrac{c\vartheta(m+1)}{2}}x^{(m-1)/2}\left[f(\eta,\tau)+\dfrac{m-1}{m+1}\eta f'(\eta,\tau)\right] \\ u = cx^m f'(\eta,\tau),\quad \eta = y\sqrt{\dfrac{c(m+1)}{2\vartheta}}x^{(m-1)/2} \\ \theta(\eta,\tau) = (T-T_\infty)/(T_w-T_\infty),\quad \tau = cx^{m-1}t \end{cases} \tag{14}$$

By substituting Eq. (14) into Eqs. (12) and (13), we get

$$\begin{aligned} &\xi_1\frac{\partial^3 f}{\partial^3\eta} + f\frac{\partial^2 f}{\partial^2\eta} - \frac{2m}{(m+1)}\left(\frac{\partial f}{\partial\eta}\right)^2 \\ &-\frac{2}{m+1}\left[1+(m-1)\tau\frac{\partial f}{\partial\eta}\right]\frac{\partial^2 f}{\partial\eta\partial\tau} = 0 \end{aligned} \tag{15}$$

$$\begin{cases} \xi_1 = \dfrac{1}{(1-\phi_{Cu})^{2.5}(1-\phi_{Al_2O_3})^{2.5}\{(1-\phi_{Al_2O_3})[1-\phi_{Cu}+\phi_{Cu}(\rho_{Cu}/\rho_f)]+\phi_{Al_2O_3}(\rho_{Al_2O_3}/\rho_f)\}} \\ \xi_2 = \dfrac{(k_{hnf}/k_f)}{\left\{(1-\phi_{Al_2O_3})\left[1-\phi_{Cu}+\phi_{Cu}\dfrac{(\rho c_p)_{Cu}}{(\rho c_p)_f}\right]+\phi_{Al_2O_3}\dfrac{(\rho c_p)_{Al_2O_3}}{(\rho c_p)_f}\right\}} \\ \xi_3 = \dfrac{1}{(1-\phi_{Cu})^{2.5}(1-\phi_{Al_2O_3})^{2.5}\left\{(1-\phi_{Al_2O_3})\left[1-\phi_{Cu}+\phi_{Cu}\dfrac{(\rho c_p)_{Cu}}{(\rho c_p)_f}\right]+\phi_{Al_2O_3}\dfrac{(\rho c_p)_{Al_2O_3}}{(\rho c_p)_f}\right\}} \end{cases} \tag{9}$$

Please cite this article in press as: Lund LA, et al. Stability analysis and multiple solution of Cu–Al_2O_3/H_2O nanofluid contains hybrid nanomaterials over a shrinking surface in the presence of viscous dissipation. J Mater Res Technol. 2019. https://doi.org/10.1016/j.jmrt.2019.10.071

$$\frac{\xi_2}{Pr}\frac{\partial^2\theta}{\partial^2\eta}+\theta' f-\frac{4m}{(m+1)}\theta\frac{\partial f}{\partial\eta}+\xi_3 Ec\left(\frac{\partial^2 f}{\partial^2\eta}\right)^2 -\frac{2}{m+1}\left[1+(m-1)\tau\frac{\partial f}{\partial\eta}\right]\frac{\partial\theta}{\partial\tau}=0 \tag{16}$$

Subject to boundary conditions

$$\begin{cases} f(0,\tau)=-b\sqrt{\dfrac{2}{m+1}},\quad \dfrac{\partial f(0,\tau)}{\partial\eta}=-1,\theta(0,\tau)=1 \\ \dfrac{\partial f(\eta,\tau)}{\partial\eta}\to 0,\theta(\eta,\tau)\to 0 \text{ as } \eta\to\infty \end{cases} \tag{17}$$

To obtain the steady flow solution's stability $f(\eta)=f_0(\eta)$, and $\theta(\eta)=\theta_0(\eta)$ satisfying Eqs. (6) and (7), we have these functions (refer [70–74])

$$\begin{cases} f(\eta,\tau)=f_0(\eta)+e^{-\gamma\tau}F(\eta,\tau) \\ \theta(\eta,\tau)=\theta_0(\eta)+e^{-\gamma\tau}G(\eta,\tau) \end{cases} \tag{18}$$

where $F(\eta,\tau)$ and $G(\eta,\tau)$ are the small relative with $f_0(\eta)$, $\theta_0(\eta)$ and γ is an unknown eigenvalue parameter. It should be noted that there are an infinite set of eigenvalues $\gamma_1<\gamma_2<\gamma_3\ldots$ By putting Eq. (18) into Eqs. (15) and (16) subject to the boundary conditions (17), we get the following linear eigenvalue problem

$$\xi_1\frac{\partial^3 F}{\partial\eta^3}+f_0\frac{\partial^2 F}{\partial\eta^2}+F\frac{d^2 f_0}{d\eta^2}-\frac{4m}{(m+1)}\frac{df_0}{d\eta}\frac{\partial F}{\partial\eta} +\frac{2}{m+1}\left[1+(m-1)\tau\frac{df_0}{d\eta}\right]\gamma\frac{\partial F}{\partial\eta}=0 \tag{19}$$

$$\frac{\xi_2}{Pr}\frac{\partial^2 G}{\partial\eta^2}+\frac{d\theta_0}{d\eta}F+\frac{\partial G}{\partial\eta}f_0-\frac{4m}{(m+1)}\left(\theta_0\frac{dF}{d\eta}+G\frac{df_0}{d\eta}\right) +2Ec\xi_3\frac{d^2 f_0}{d\eta^2}\frac{\partial^2 F}{\partial\eta^2} +\frac{2}{m+1}\left[1+(m-1)\tau\frac{df_0}{d\eta}\right]\gamma G=0 \tag{20}$$

We follow the Weidman et al. [75] and keep $\tau=0$, and $F=F_0$ and $G=G_0$ in Eqs. (19) and (20) in order to determine the initial growth or decay of solutions. Henceforth, we get following linearized eigenvalues problems

$$\xi_1 F'''_0+f_0F'''_0+F_0f''_0+\frac{2}{m+1}(\gamma-2mf'_0)F'_0=0 \tag{21}$$

$$\frac{\xi_2}{Pr}G''_0+\theta'_0F_0+G'_0f_0+2Ec\xi_3 f''_0F''_0-\frac{4m}{(m+1)}\theta_0F'_0 +\frac{2}{m+1}(\gamma-2mf'_0)G_0=0 \tag{22}$$

Subject to corresponding boundary conditions

$$\begin{cases} F_0(0)=0,\ F'_0(0)=0,\ G_0(0)=0 \\ F'_0(\eta)\to 0,\ G_0(\eta)\to 0 \text{ as } \eta\to\infty \end{cases} \tag{23}$$

Table 3 – The compression of results ($f''(0)$) of present numerical method with Yasin et al. [76].

m	b	Exact solutions		Present results	
		1st solution	2nd solution	1st solution	2nd solution
1	−2	1	–	1.0001	–
	−3	2.61803	0.38197	2.61803	0.38195
	−4	3.37205	0.26795	3.73205	0.26795
1.5	−3	–	–	2.18308	0.11939
2.5	−3	–	–	1.47109	0.49794

Table 4 – The compression of $\sqrt{Re}C_f$ with Devi and Devi [61] and Waini et al. [62].

m	ϕ_{Cu}	Devi and Devi [61]	Waini et al. [62]	Present results
1	0.005	−1.327310	−1.327098	−1.325862
	0.02	−1.409683	−1.409490	−1.404648
	0.04	−1.520894	−1.520721	−1.511257
	0.06	−1.634279	−1.634119	−1.620177
1.5	0.02	–	–	−1.491175
	0.04	–	–	−1.604352
2.5	0.02	–	–	−1.585037
	0.04	–	–	1.705327

In order to get values of the smallest eigenvalue, we solved Eqs. (21) and (22) subject to boundary conditions (23). The signs of the smallest eigenvalue predict that either flow is stable or not. If the sign of the smallest eigenvalue is positive (negative) then flow is said to be stable (unstable).

4. Results and discussion

The system of transformed ODEs (6) and (7) along with corresponding boundary conditions (8) has been solved numerically by employing a three-stage Lobatto IIIa formula with the help of the MATLAB software for various values of the nanoparticle volume fractions $\phi_{Al_2O_3}$, ϕ_{Cu}, suction/injection parameter S and Eckert number Ec. It is worth to highlight that when $\phi_{Al_2O_3}=\phi_{Cu}=0$ then our Eq. (6) is reduced to a simple viscous fluid case. The exact solutions of the reduced equation are already given in the paper of Yasin et al. [76] (see Eq. (22)). Further, the results of the present study are compared to the results of Yasin et al. [76] in Table 3 and found in excellent agreement. Table 4 is also constructed in order to validate the results of the coefficient of skin friction for Al_2O_3-Cu/H_2O hybrid nanofluid for different values of ϕ_{Cu} when $\phi_{Al_2O_3}=0.1$, $S=0$, $Pr=6.135$, for stretching surface ($f'(0)=1$) with Waini et al. [62] and Devi and Devi [61]. For other properties of the fluid and solid, we follow the Devi and Devi [61] in which $\rho_f=997$, $c_{pf}=4180$, $k_f=0.607$. The present results show a favorable agreement with those gotten by Waini et al. [62] and Devi and Devi [61]. The results of the present study for the coefficient of skin friction and heat transfer rate are given in Table 5.

Variation of $f''(0)$ with suction/injection parameter b and volume fraction parameter $\phi_{Al_2O_3}$ for base fluid water was drawn in Fig. 2. The skin friction coefficient advances for small values of $\phi_{Al_2O_3}$ and increasing behavior is noticed for lower values of suction parameter b in the first solution. Physically, suction produces more resistance in the fluid flow and therefore the coefficient of skin friction decreases in the sta-

Please cite this article in press as: Lund LA, et al. Stability analysis and multiple solution of Cu–Al_2O_3/H_2O nanofluid contains hybrid nanomaterials over a shrinking surface in the presence of viscous dissipation. J Mater Res Technol. 2019. https://doi.org/10.1016/j.jmrt.2019.10.071

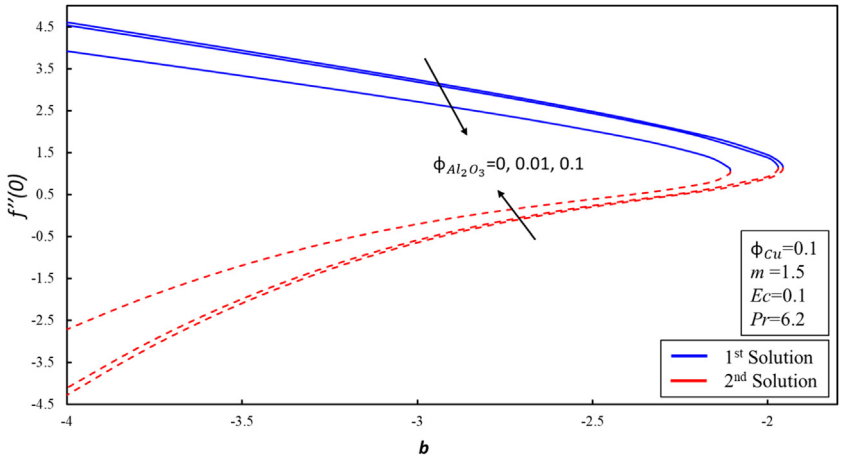

Fig. 2 – Variation of $f''(0)$ for various values of b.

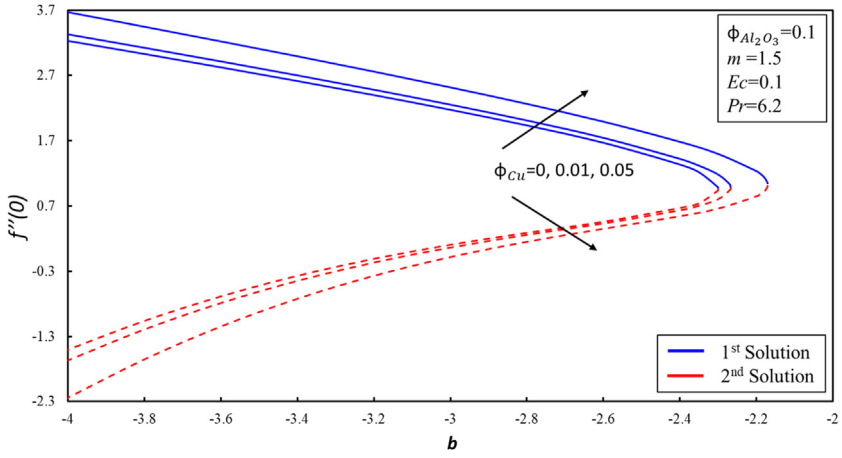

Fig. 3 – Variation of $f''(0)$ for various values of b.

Table 5 – The results of $f''(0)$ and $-\theta'(0)$ over the shrinking surface where $Pr = 6.2$ and $b = -3$.

m	Ec	ϕ_{Cu}	$\phi_{Al_2O_3}$	$f''(0)$	$-\theta'(0)$
1	**0.1**	**0**	**0.05**	2.65107872	14.1234276
1	0.1	**0.01**	0.05	2.77281027	13.6122442
1	0.1	**0.05**	0.05	3.17252159	11.7696479
1	0.1	**0.1**	0.05	3.49494958	9.84447959
1	0.1	0.1	**0**	3.77446217	11.6647986
1	0.1	0.1	**0.1**	3.19641917	8.33053511
1	**0**	0.1	0.1	3.19641917	9.37865329
1.5	0	0.1	0.1	2.71203378	8.03940995
1.5	**0.1**	0.1	0.1	2.71203378	7.09939876
2.5	0.1	**0.05**	0.1	1.80512347	6.44830162
2.5	0.1	0.05	**0.05**	1.96672019	7.85309519

Bold values shows variations in that parameter.

ble solution. On the other hand, the opposite behavior is noticed for the second solution. It is worth noticing that there is a range of dual solutions and no solution which depends upon the critical values where dual solutions exist. When $\phi_{Al_2O_3} = 0$, 0.01, and 0.1, the respective dual solutions ranges are $b \leq -1.9561$, -1.9686, and -2.1066. Fig. 3 demonstrates the variation of $f''(0)$ with b for various values of ϕ_{Cu}. It can be noticed that the critical values b ($b \leq -2.2995$) for the Al_2O_3 water-based nanofluid is a bit lesser than the critical values b ($b \leq -2.267$ for $\phi_{Cu} = 0.01$; $b \leq -2.1713$ for $\phi_{Cu} = 0.05$) for the hybrid nanofluid. On the other hand, the $f''(0)$ increases for higher values of ϕ_{Cu} and the decreasing trend can be seen for lower values of the suction parameter b in the first solution. On the other hand, the opposite behavior is noticed for the second solutions.

Variations of $-\theta'(0)$ with b for increasing values of $\phi_{Al_2O_3}$ and ϕ_{Cu} are plotted in Figs. 4 and 5 respectively. From these plots, it can be observed that the rate of heat transfer reduces in both solutions. This reduction helps the fluid to transfer coolant easily inside the boundary layer and therefore, the temperature of fluid decreases. The profile of velocity $f'(\eta)$ for several values of m is revealed in Fig. 6. This figure displays that there are two distinct profiles of the velocity of fluid for the various values of non-negative constant. It is observed that when $m = 0$, there exists only a single solution. It is noticed that the enhancing of m leads to the rise of the velocity of hybrid nanofluid in the first solution, while opposite trend is noticed in the second solution. On the other hand,

Please cite this article in press as: Lund LA, et al. Stability analysis and multiple solution of Cu–Al_2O_3/H_2O nanofluid contains hybrid nanomaterials over a shrinking surface in the presence of viscous dissipation. J Mater Res Technol. 2019. https://doi.org/10.1016/j.jmrt.2019.10.071

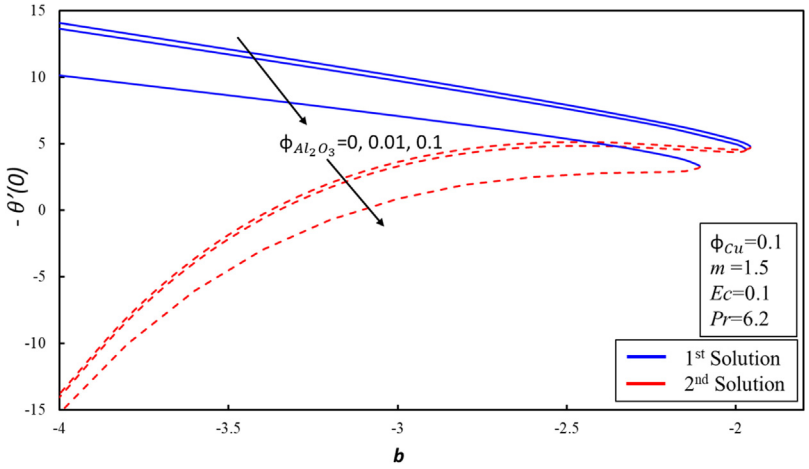

Fig. 4 – Variation of $-\theta'(0)$ for various values of b.

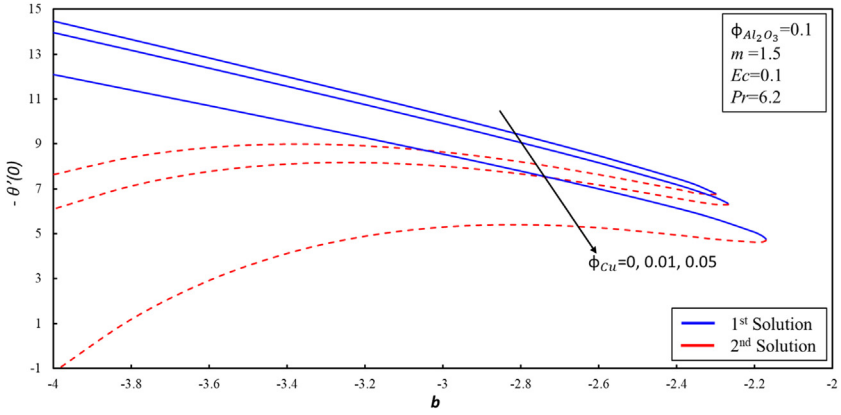

Fig. 5 – Variation of $-\theta'(0)$ for various values of b.

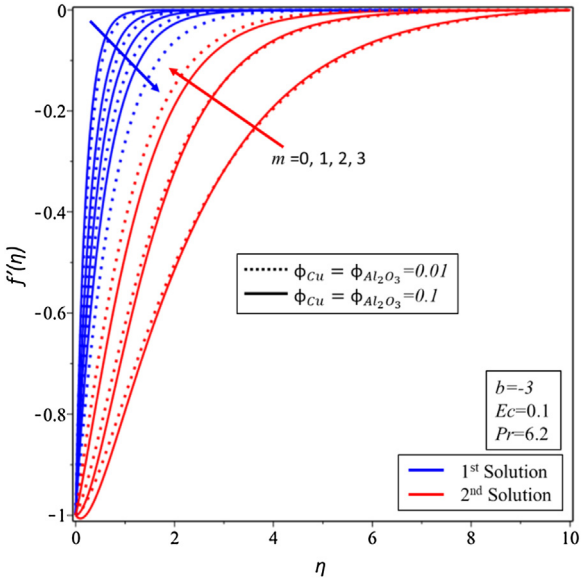

Fig. 6 – Variation of $f'(\eta)$ for various values of m.

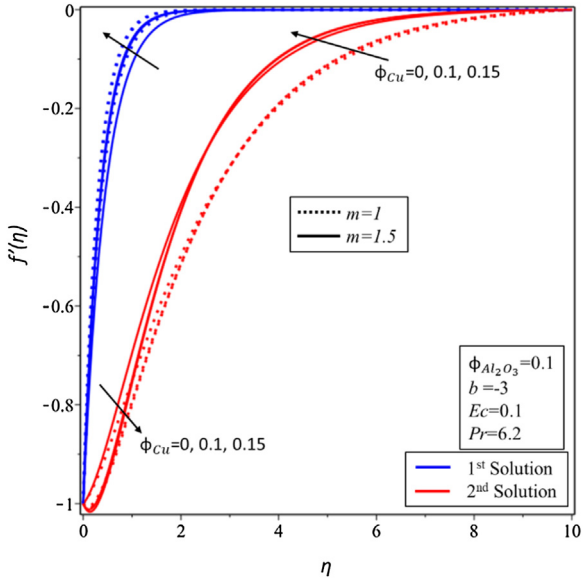

Fig. 7 – Variation of $f'(\eta)$ for various values of ϕ_{Cu}.

Please cite this article in press as: Lund LA, et al. Stability analysis and multiple solution of Cu–Al_2O_3/H_2O nanofluid contains hybrid nanomaterials over a shrinking surface in the presence of viscous dissipation. J Mater Res Technol. 2019. https://doi.org/10.1016/j.jmrt.2019.10.071

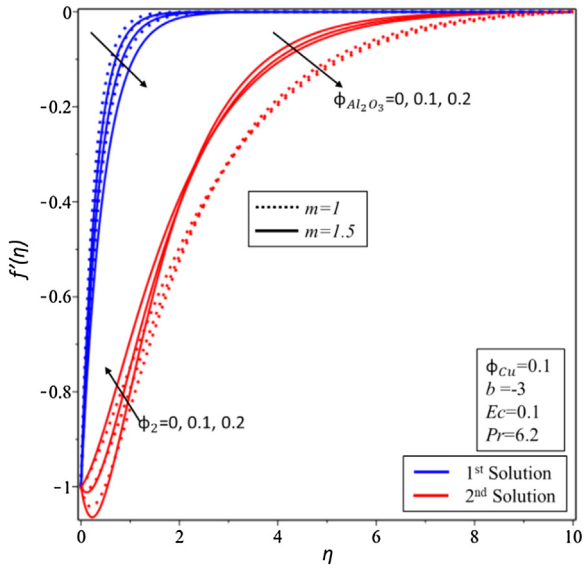

Fig. 8 – Variation of $f'(\eta)$ for various values of $\phi_{Al_2O_3}$.

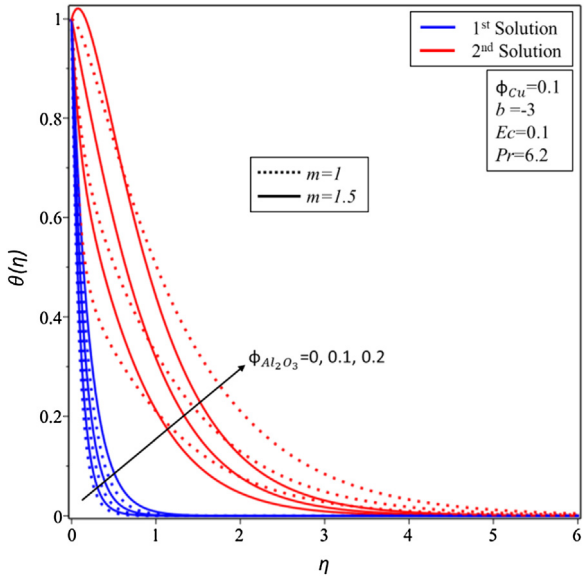

Fig. 10 – Variation of $\theta(\eta)$ for various values of $\phi_{Al_2O_3}$.

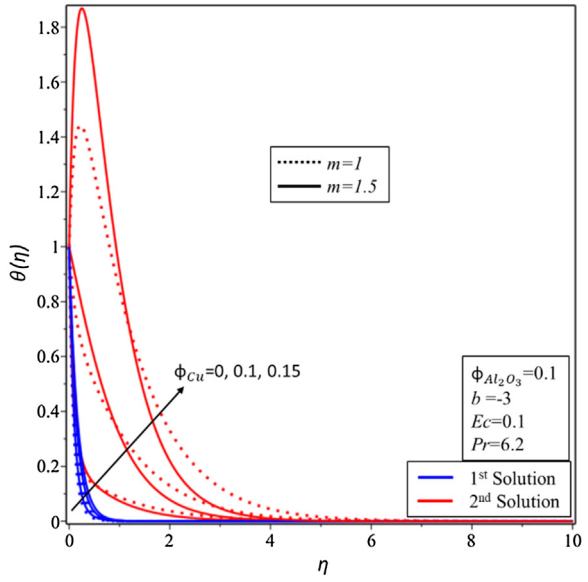

Fig. 9 – Variation of $\theta(\eta)$ for various values of ϕ_{Cu}.

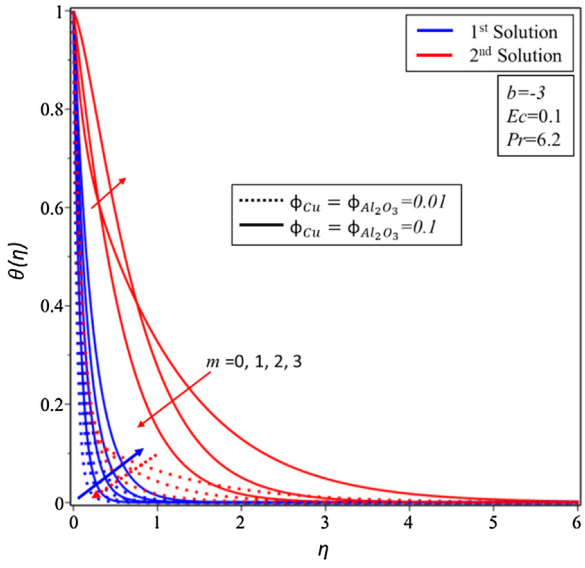

Fig. 11 – Variation of $\theta(\eta)$ for various values of m.

velocity distributions of $\phi_{Al_2O_3} = \phi_{Cu} = 0.01$ are higher than the $\phi_{Al_2O_3} = \phi_{Cu} = 0.1$. The profile of velocity for Cu–Al_2O_3/water hybrid nanofluid is sketched in Fig. 7. It is noticed that the fluid velocity boundary layer thickness is higher for the non-linear surface in a stable solution as expected. The velocity profile demonstrates a declining nature for higher values of ϕ_{Cu} in the first solution. However, the increasing and decreasing behavior of the velocity profile is found in the second solution, the same behavior of velocity profile is examined in Fig. 8 when we checked the effect of $\phi_{Al_2O_3}$. For the first solution, the thickness of the velocity boundary layer improves for the influence of nanoparticle volume fraction $\phi_{Al_2O_3}$. Practically, this is because a higher nanoparticle volume fraction $\phi_{Al_2O_3}$ parameter produces less skin friction and as a resulting thickness of the velocity boundary layer and velocity of hybrid nanofluid flow increase.

Fig. 9 exhibits the variation of nanoparticle volume fraction ϕ_{Cu} on the distribution of temperature for linear and non-linear cases. The higher value of ϕ_{Cu} reduces the convective heat transfer and as a result, heat is transferred from heated fluid to hot surface due to which temperature increases in both solutions. The same behavior is noticed in both solutions when the effect of nanoparticle volume fraction $\phi_{Al_2O_3}$ is checked in temperature profile in Fig. 10. Fig. 11 is sketched for temperature distribution for the influence of the power index m. The thickness of the thermal boundary layer enhances for a stable solution when m is increased, while the dual behavior of temperature is found in the second solution. It is worth mentioning that thickness of thermal boundary layer is lesser when $\phi_{Al_2O_3} = \phi_{Cu} = 0.01$ which means that a large amount of heat transfer is possible as compared to $\phi_{Al_2O_3} = \phi_{Cu} = 0.1$. The influence of a Eckert number Ec on temperature profile

Please cite this article in press as: Lund LA, et al. Stability analysis and multiple solution of Cu–Al_2O_3/H_2O nanofluid contains hybrid nanomaterials over a shrinking surface in the presence of viscous dissipation. J Mater Res Technol. 2019. https://doi.org/10.1016/j.jmrt.2019.10.071

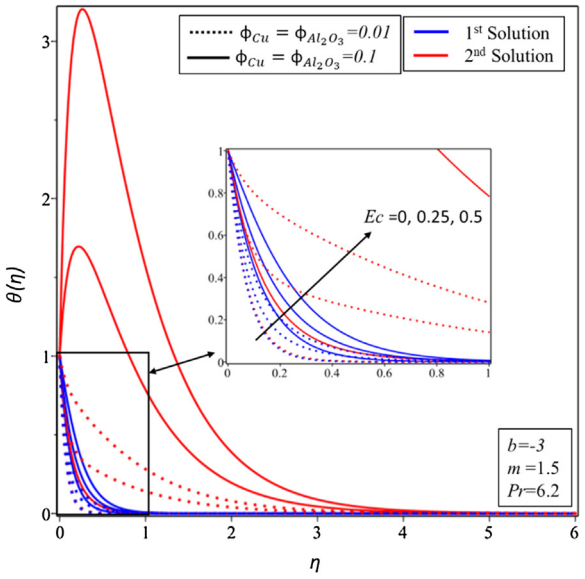

Fig. 12 – Variation of $\theta(\eta)$ for various values of Ec.

$\theta(\eta)$ is revealed in Fig. 12. The thermal boundary layer thickness and temperature rise in both solutions. Practically, this rise of temperature because of the lower effect of enthalpy difference because Eckert number is the ratio of the kinetic energy flow and an enthalpy difference of boundary layer. It advances the converting of kinetic energy into internal energy by differing fluid stresses. It is worth to mention that cooling of the surface or in other words loss of temperature from the surface to the fluid flow is possible for $0 < Ec \ll 1$.

For several values of b, the values of the smallest eigenvalue γ have been taken and demonstrated graphically in Fig. 13. This figure shows that positive values of γ denote to a disturbance initial decay and the flow becomes stable. On the other hand, the negative value of γ represents a disturbance initial growth and the flow is known as in a stable flow. It can be noticed that the values of the smallest eigenvalue γ approach to zero from both solutions as the values of b are tending to b_c.

5. Conclusion

The steady flow of Cu–Al_2O_3/water hybrid nanofluid on a non-linear shrinking sheet of variable thickness is examined with the effect of viscous dissipation. With the help of Tiwari and Das's model, the system of governing equations of hybrid nanofluid is taken. The system of PDEs is changed to a system of non-linear ODEs by employing similarity transformations. The resultant boundary value problems of ODEs have been solved by using BVP4C in MATLAB. Derivations of equations of stability analysis also have been done. The key points of this study can be presented as follows.

1. The flow in the first solution accelerates for increasing values of volume fraction parameter $\phi_{Al_2O_3}$. Further, velocity of fluid increases more when $m > 1$ as compared to $m \leq 1$. Velocity of fluid decelerates for the stable solution for higher values of volume fraction parameter ϕ_{Cu}.
2. Increasing volume fraction (ϕ_{Cu} and $\phi_{Al_2O_3}$) decreases the heat transfer rate in both solutions.
3. At high Prandtl number, the thickness of thermal boundary layer decreases in both solutions of hybrid nanofluid as expected.
4. Profile of temperature profile $\theta(\eta)$ increases in both solutions for advance values volume fraction parameters ϕ_{Cu}, $\phi_{Al_2O_3}$ and Eckert number Ec.
5. Dual solutions exist in the ranges of suction/injection parameter.
6. Only first solution can be visualized and is said be stable solution.

Conflicts of interest

The authors declare no conflicts of interest.

Acknowledgments

The authors would like to extend their sincere appreciation to the Deanship of Scientific Research at King Saud University for its funding of this research through Research Group Project

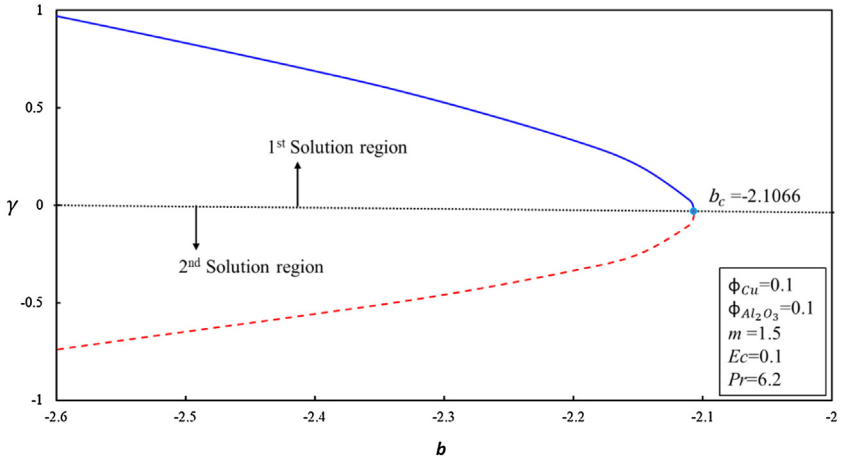

Fig. 13 – Smallest eigenvalues γ for various values of b.

Please cite this article in press as: Lund LA, et al. Stability analysis and multiple solution of Cu–Al_2O_3/H_2O nanofluid contains hybrid nanomaterials over a shrinking surface in the presence of viscous dissipation. J Mater Res Technol. 2019. https://doi.org/10.1016/j.jmrt.2019.10.071

No. RG-1439-029. This research is also supported by Universiti Utara Malaysia.

REFERENCES

[1] Choi SU, Eastman JA. Enhancing thermal conductivity of fluids with nanoparticles (No. ANL/MSD/CP-84938; CONF-951135-29). IL (United States): Argonne National Lab; 1995.
[2] Gherasim I, Roy G, Nguyen CT, Vo-Ngoc D. Experimental investigation of nanofluids in confined laminar radial flows. Int J Therm Sci 2009;48(8):1486–93.
[3] Chandrasekar M, Suresh S, Bose AC. Experimental investigations and theoretical determination of thermal conductivity and viscosity of Al_2O_3/water nanofluid. Exp Therm Fluid Sci 2010;34(2):210–6.
[4] Yu W, Xie H, Chen W. Experimental investigation on thermal conductivity of nanofluids containing graphene oxide nanosheets. J Appl Phys 2010;107(9):094317.
[5] Dalkılıç AS, Türk OA, Mercan H, Nakkaew S, Wongwises S. An experimental investigation on heat transfer characteristics of graphite–SiO_2/water hybrid nanofluid flow in horizontal tube with various quad-channel twisted tape inserts. Int Commun Heat Mass Transf 2019;107:1–13.
[6] Akhgar A, Toghraie D. An experimental study on the stability and thermal conductivity of water–ethylene glycol/TiO_2–MWCNTs hybrid nanofluid: developing a new correlation. Powder Technol 2018;338:806–18.
[7] Esfahani MA, Toghraie D. Experimental investigation for developing a new model for the thermal conductivity of silica/water–ethylene glycol (40%–60%) nanofluid at different temperatures and solid volume fractions. J Mol Liq 2017;232:105–12.
[8] Barnoon P, Toghraie D. Numerical investigation of laminar flow and heat transfer of non-Newtonian nanofluid within a porous medium. Powder Technol 2018;325:78–91.
[9] Esfe MH, Hajmohammad H, Toghraie D, Rostamian H, Mahian O, Wongwises S. Multi-objective optimization of nanofluid flow in double tube heat exchangers for applications in energy systems. Energy 2017;137:160–71.
[10] Heydari M, Toghraie D, Akbari OA. The effect of semi-attached and offset mid-truncated ribs and water/TiO_2 nanofluid on flow and heat transfer properties in a triangular microchannel. Therm Sci Eng Prog 2017;2:140–50.
[11] Jamali M, Toghraie D. Investigation of heat transfer characteristics in the developing and the developed flow of nanofluid inside a tube with different entrances in the transition regime. J Therm Anal Calorim 2019:1–15.
[12] Khodabandeh E, Bahiraei M, Mashayekhi R, Talebjedi B, Toghraie D. Thermal performance of Ag–water nanofluid in tube equipped with novel conical strip inserts using two-phase method: geometry effects and particle migration considerations. Powder Technol 2018;338:87–100.
[13] Khodabandeh E, Rozati SA, Joshaghani M, Akbari OA, Akbari S, Toghraie D. Thermal performance improvement in water nanofluid/GNP–SDBS in novel design of double-layer microchannel heat sink with sinusoidal cavities and rectangular ribs. J Therm Anal Calorim 2019;136(3):1333–45.
[14] Mashayekhi R, Khodabandeh E, Bahiraei M, Bahrami L, Toghraie D, Akbari OA. Application of a novel conical strip insert to improve the efficacy of water–Ag nanofluid for utilization in thermal systems: a two-phase simulation. Energy Convers Manage 2017;151:573–86.
[15] Pourfattah F, Motamedian M, Sheikhzadeh G, Toghraie D, Akbari OA. The numerical investigation of angle of attack of inclined rectangular rib on the turbulent heat transfer of water–Al_2O_3 nanofluid in a tube. Int J Mech Sci 2017;131:1106–16.
[16] Rezaei O, Akbari OA, Marzban A, Toghraie D, Pourfattah F, Mashayekhi R. The numerical investigation of heat transfer and pressure drop of turbulent flow in a triangular microchannel. Phys E: Low Dimen Syst Nanostruct 2017;93:179–89.
[17] Saeedi AH, Akbari M, Toghraie D. An experimental study on rheological behavior of a nanofluid containing oxide nanoparticle and proposing a new correlation. Phys E: Low Dimens Syst Nanostruct 2018;99:285–93.
[18] Sarlak R, Yousefzadeh S, Akbari OA, Toghraie D, Sarlak S. The investigation of simultaneous heat transfer of water/Al_2O_3 nanofluid in a close enclosure by applying homogeneous magnetic field. Int J Mech Sci 2017;133:674–88.
[19] Varzaneh AA, Toghraie D, Karimipour A. Comprehensive simulation of nanofluid flow and heat transfer in straight ribbed microtube using single-phase and two-phase models for choosing the best conditions. J Therm Anal Calorim 2019:1–20.
[20] Tiwari RK, Das MK. Heat transfer augmentation in a two-sided lid-driven differentially heated square cavity utilizing nanofluids. Int J Heat Mass Transfer 2007;50(9–10):2002–18.
[21] Buongiorno J. Convective transport in nanofluids. J Heat Transfer 2006;128(3):240–50.
[22] Hayat T, Khan MI, Waqas M, Alsaedi A, Farooq M. Numerical simulation for melting heat transfer and radiation effects in stagnation point flow of carbon–water nanofluid. Comput Methods Appl Mech Eng 2017;315:1011–24.
[23] Alrashed AA, Akbari OA, Heydari A, Toghraie D, Zarringhalam M, Shabani GAS, et al. The numerical modeling of water/FMWCNT nanofluid flow and heat transfer in a backward-facing contracting channel. Phys B: Condens Matter 2018;537:176–83.
[24] Rashid I, Sagheer M, Hussain S. Entropy formation analysis of MHD boundary layer flow of nanofluid over a porous shrinking wall. Phys A: Stat Mech Appl 2019:122608.
[25] Sivasankaran S, Alsabery AI, Hashim I. Internal heat generation effect on transient natural convection in a nanofluid-saturated local thermal non-equilibrium porous inclined cavity. Phys A: Stat Mech Appl 2018;509:275–93.
[26] Nguyen-Thoi T, Sheikholeslami M, Hamid M, Haq RU, Shafee A. CVFEM modeling for nanofluid behavior involving non-equilibrium model and Lorentz effect in appearance of radiation. Phys A: Stat Mech Appl 2019;534:122154.
[27] Sheremet MA, Pop I, Bachok N. Effect of thermal dispersion on transient natural convection in a wavy-walled porous cavity filled with a nanofluid: Tiwari and Das' nanofluid model. Int J Heat Mass Transfer 2016;92:1053–60.
[28] Sheremet MA, Pop I, Mahian O. Natural convection in an inclined cavity with time-periodic temperature boundary conditions using nanofluids: application in solar collectors. Int J Heat Mass Transfer 2018;116:751–61.
[29] Dinarvand S, Pop I. Free-convective flow of copper/water nanofluid about a rotating down-pointing cone using Tiwari-Das nanofluid scheme. Adv Powder Technol 2017;28(3):900–9.
[30] Aghamajidi M, Yazdi M, Dinarvand S, Pop I. Tiwari-Das nanofluid model for magnetohydrodynamics (MHD) natural-convective flow of a nanofluid adjacent to a spinning down-pointing vertical cone. Propul Power Res 2018;7(1):78–90.
[31] Hussanan A, Salleh MZ, Khan I, Chen ZM. Unsteady water functionalized oxide and non-oxide nanofluids flow over an infinite accelerated plate. Chin J Phys 2019.
[32] Sheikh NA, Ali F, Khan I, Gohar M. A theoretical study on the performance of a solar collector using CeO_2 and Al_2O_3 water

Please cite this article in press as: Lund LA, et al. Stability analysis and multiple solution of Cu–Al_2O_3/H_2O nanofluid contains hybrid nanomaterials over a shrinking surface in the presence of viscous dissipation. J Mater Res Technol. 2019. https://doi.org/10.1016/j.jmrt.2019.10.071

based nanofluids with inclined plate: Atangana–Baleanu fractional model. Chaos Soliton Fract 2018;115:135–42.
[33] Hayat T, Khan MI, Qayyum S, Alsaedi A. Entropy generation in flow with silver and copper nanoparticles. Colloids Surf A: Physicochem Eng Asp 2018;539:335–46.
[34] Hayat T, Khan MI, Farooq M, Alsaedi A, Yasmeen T. Impact of Marangoni convection in the flow of carbon–water nanofluid with thermal radiation. Int J Heat Mass Transfer 2017;106:810–5.
[35] Qayyum S, Khan MI, Hayat T, Alsaedi A. A framework for nonlinear thermal radiation and homogeneous–heterogeneous reactions flow based on silver–water and copper–water nanoparticles: a numerical model for probable error. Results Phys 2017;7:1907–14.
[36] Farooq M, Khan MI, Waqas M, Hayat T, Alsaedi A, Khan MI. MHD stagnation point flow of viscoelastic nanofluid with non-linear radiation effects. J Mol Liq 2016;221:1097–103.
[37] Khan MI, Hayat T, Khan MI, Alsaedi A. Activation energy impact in nonlinear radiative stagnation point flow of Cross nanofluid. Int Commun Heat Mass Transf 2018;91:216–24.
[38] Hayat T, Khan MI, Farooq M, Alsaedi A, Waqas M, Yasmeen T. Impact of Cattaneo–Christov heat flux model in flow of variable thermal conductivity fluid over a variable thicked surface. Int J Heat Mass Transfer 2016;99:702–10.
[39] Hayat T, Muhammad K, Farooq M, Alsaedi A. Squeezed flow subject to Cattaneo–Christov heat flux and rotating frame. J Mol Liq 2016;220:216–22.
[40] Hayat T, Waqas M, Khan MI, Alsaedi A. Analysis of thixotropic nanomaterial in a doubly stratified medium considering magnetic field effects. Int J Heat Mass Transfer 2016;102:1123–9.
[41] Hayat T, Khan MI, Waqas M, Alsaedi A. Mathematical modeling of non-Newtonian fluid with chemical aspects: a new formulation and results by numerical technique. Colloids Surf A: Physicochem Eng Asp 2017;518:263–72.
[42] Hayat T, Khan MI, Farooq M, Alsaedi A, Khan MI. Thermally stratified stretching flow with Cattaneo–Christov heat flux. Int J Heat Mass Transfer 2017;106:289–94.
[43] Hayat T, Qayyum S, Khan MI, Alsaedi A. Entropy generation in magnetohydrodynamic radiative flow due to rotating disk in presence of viscous dissipation and Joule heating. Phys Fluids 2018;30(1):017101.
[44] Hayat T, Khan MI, Waqas M, Alsaedi A, Khan MI. Radiative flow of micropolar nanofluid accounting thermophoresis and Brownian moment. Int J Hydrogen Energy 2017;42(26):16821–33.
[45] Khan MI, Waqas M, Hayat T, Khan MI, Alsaedi A. Behavior of stratification phenomenon in flow of Maxwell nanomaterial with motile gyrotactic microorganisms in the presence of magnetic field. Int J Mech Sci 2017;131:426–34.
[46] Khan MI, Waqas M, Hayat T, Alsaedi A. A comparative study of Casson fluid with homogeneous–heterogeneous reactions. J Colloid Interface Sci 2017;498:85–90.
[47] Khan MI, Hayat T, Khan MI, Alsaedi A. A modified homogeneous–heterogeneous reactions for MHD stagnation flow with viscous dissipation and Joule heating. Int J Heat Mass Transfer 2017;113:310–7.
[48] Rasool G, Zhang T. Darcy-Forchheimer nanofluidic flow manifested with Cattaneo-Christov theory of heat and mass flux over non-linearly stretching surface. PloS One 2019;14(8):e0221302.
[49] Khan SU, Rauf A, Shehzad SA, Abbas Z, Javed T. Study of bioconvection flow in Oldroyd-B nanofluid with motile organisms and effective Prandtl approach. Phys A: Stat Mech Appl 2019;527:121179.
[50] Lund LA, Omar Z, Khan I. Mathematical analysis of magnetohydrodynamic (MHD) flow of micropolar nanofluid under buoyancy effects past a vertical shrinking surface: dual solutions. Heliyon 2019;5(9):e02432.
[51] Ullah I, Shafie S, Makinde OD, Khan I. Unsteady MHD Falkner-Skan flow of Casson nanofluid with generative/destructive chemical reaction. Chem Eng Sci 2017;172:694–706.
[52] Rasool G, Zhang T, Shafiq A. Second grade nanofluidic flow past a convectively heated vertical Riga plate. Phys Scr 2019.
[53] Lund LA, Omar Z, Khan I. Quadruple solutions of mixed convection flow of magnetohydrodynamic nanofluid over exponentially vertical shrinking and stretching surfaces: stability analysis. Comput Methods Prog Biomed 2019;182:105044.
[54] Sheremet MA, Cimpean DS, Pop I. Free convection in a partially heated wavy porous cavity filled with a nanofluid under the effects of Brownian diffusion and thermophoresis. Appl Therm Eng 2017;113:413–8.
[55] Hayat T, Ahmad S, Khan MI, Alsaedi A. Simulation of ferromagnetic nanomaterial flow of Maxwell fluid. Results Phys 2018;8:34–40.
[56] Hayat T, Khan MI, Qayyum S, Alsaedi A, Khan MI. New thermodynamics of entropy generation minimization with nonlinear thermal radiation and nanomaterials. Phys Lett A 2018;382(11):749–60.
[57] Khan MWA, Khan MI, Hayat T, Alsaedi A. Entropy generation minimization (EGM) of nanofluid flow by a thin moving needle with nonlinear thermal radiation. Phys B: Condens Matter 2018;534:113–9.
[58] Sheikholeslami M, Mehryan SAM, Shafee A, Sheremet MA. Variable magnetic forces impact on magnetizable hybrid nanofluid heat transfer through a circular cavity. J Mol Liq 2019;277:388–96.
[59] Arasteh H, Mashayekhi R, Toghraie D, Karimipour A, Bahiraei M, Rahbari A. Optimal arrangements of a heat sink partially filled with multilayered porous media employing hybrid nanofluid. J Therm Anal Calorim 2019:1–14.
[60] Devi SA, Devi SSU. Numerical investigation of hydromagnetic hybrid Cu–Al_2O_3/water nanofluid flow over a permeable stretching sheet with suction. Int J Nonlin Sci Numer Simul 2016;17(5):249–57.
[61] Devi SU, Devi SA. Heat transfer enhancement of Cu–Al_2O_3/water hybrid nanofluid flow over a stretching sheet. J Nigerian Math Soc 2017;36(2):419–33.
[62] Waini I, Ishak A, Pop I. Unsteady flow and heat transfer past a stretching/shrinking sheet in a hybrid nanofluid. Int J Heat Mass Transfer 2019;136:288–97.
[63] Waini I, Ishak A, Pop I. Hybrid nanofluid flow and heat transfer past a vertical thin needle with prescribed surface heat flux. Int J Numer Methods Heat Fluid Flow 2019.
[64] Merkin JH. Mixed convection boundary layer flow on a vertical surface in a saturated porous medium. J Eng Math 1980;14(4):301–13.
[65] Lund LA, Omar Z, Khan I. Steady incompressible magnetohydrodynamics Casson boundary layer flow past a permeable vertical and exponentially shrinking sheet: a stability analysis. Heat Transf—Asian Res 2019.
[66] Usama NS, Khan AU. Stability analysis of Cu–H_2O nanofluid over a curved stretching–shrinking sheet: existence of dual solutions. Can J Phys 2019;97(8):911–22.
[67] Awaludin IS, Ishak A, Pop I. On the stability of MHD boundary layer flow over a stretching/shrinking wedge. Sci Rep 2018;8(1):13622.
[68] Ali Lund L, Ching DLC, Omar Z, Khan I, Nisar KS. Triple local similarity solutions of Darcy-Forchheimer Magnetohydrodynamic (MHD) flow of micropolar nanofluid over an exponential shrinking surface: stability analysis. Coatings 2019;9(8):527.

Please cite this article in press as: Lund LA, et al. Stability analysis and multiple solution of Cu–Al_2O_3/H_2O nanofluid contains hybrid nanomaterials over a shrinking surface in the presence of viscous dissipation. J Mater Res Technol. 2019. https://doi.org/10.1016/j.jmrt.2019.10.071

[69] Najib N, Bachok N, Arifin N, Ali F. Stability analysis of stagnation-point flow in a nanofluid over a stretching/shrinking sheet with second-order slip, soret and dufour effects: a revised model. Appl Sci 2018;8(4):642.
[70] Tan W, Masuoka T. Stability analysis of a Maxwell fluid in a porous medium heated from below. Phys Lett A 2007;360(3):454–60.
[71] Lund LA, Omar Z, Khan I. Analysis of dual solution for MHD flow of Williamson fluid with slippage. Heliyon 2019;5(3):e01345.
[72] Mustafa I, Javed T, Ghaffari A, Khalil H. Enhancement in heat and mass transfer over a permeable sheet with Newtonian heating effects on nanofluid: multiple solutions using spectral method and stability analysis. Pramana 2019;93(4):53.
[73] Anuar NS, Bachok N, Arifin NM, Rosali H. Stagnation point flow and heat transfer over an exponentially stretching/shrinking sheet in CNT with homogeneous–heterogeneous reaction: stability analysis. Symmetry 2019;11(4):522.
[74] Alarifi IM, Abokhalil AG, Osman M, Lund LA, Ayed MB, Belmabrouk H, et al. MHD flow and heat transfer over vertical stretching sheet with heat sink or source effect. Symmetry 2019;11(3):297.
[75] Weidman PD, Kubitschek DG, Davis AMJ. The effect of transpiration on self-similar boundary layer flow over moving surfaces. Int J Eng Sci 2006;44(11–12):730–7.
[76] Yasin MHM, Ishak A, Pop I. Boundary layer flow and heat transfer past a permeable shrinking surface embedded in a porous medium with a second-order slip: a stability analysis. Appl Therm Eng 2017;115:1407–11.
[77] Saqib M, Khan I, Shafie S. Application of fractional differential equations to heat transfer in hybrid nanofluid: modeling and solution via integral transforms. Adv Difference Equ 2019;2019(1):52.
[78] Lund LA, Omar Z, Khan I, Dero S. Multiple solutions of Cu–$C_6H_9{\cdot}NaO_7$ and Ag–$C_6H_9{\cdot}NaO_7$ nanofluids flow over nonlinear shrinking surface. J Cent South Univ 2019;26(5):1283–93.

Please cite this article in press as: Lund LA, et al. Stability analysis and multiple solution of Cu–Al_2O_3/H_2O nanofluid contains hybrid nanomaterials over a shrinking surface in the presence of viscous dissipation. J Mater Res Technol. 2019. https://doi.org/10.1016/j.jmrt.2019.10.071